ACS OMEGA

http://pubs.acs.org/journal/acsodf

Article

Thermogravimetric Characteristics and Pyrolysis Kinetics of Nigerian Oil Sands

Odunayo T. Ore* and Festus M. Adebiyi

Cite This: *ACS Omega* 2023, 8, 10111−10118

Read Online

ACCESS | Metrics & More | Article Recommendations | Supporting Information

ABSTRACT: In the present study, the pyrolysis behavior of Nigerian oil sands was investigated using thermogravimetric analysis. This was done with the aim of deriving kinetic models that can be relevant in the development of the natural resource. The effects of different heating rates (10, 20, and 30 °C/min) on oil sand pyrolysis were studied. The results of the study indicated that three regions comprising low-temperature oxidation, devolatilization, and high-temperature oxidation were obtained at all heating rates. The peak temperatures were observed to rise with an increasing heating rate, a phenomenon described as thermal hysteresis. Mineralogical analysis showed the presence of diffraction peaks corresponding to chlorite, quartz, aragonite, dolomite, calcite, and montmorillonite minerals and the notable absence of expandable clay minerals which are known to pose problems during tailing management and the aqueous bitumen extraction process. The kinetic analysis showed that the activation energy increased with the degree of conversion, with the highest activation energy of 14.682 kJ mol^{-1}. The Coats−Redfern kinetic model gave the best model fit for oil sand pyrolysis.

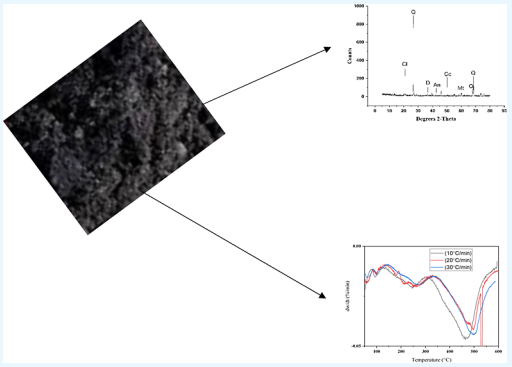

1. INTRODUCTION

There is a growing interest in the exploration of unconventional oil and gas resources due to the dearth of energy resources owing to the depleting conventional oil reserves.[1] The diminution of conventional oil reserves is brought about by the increasing energy demands of mechanization and industrialization.[2] Conventional hydrocarbon resources such as oil, natural gas, and coal can no longer satisfy the ever-increasing energy needs brought about by economic development.[3] In very recent years, significant attention has been drawn to the utilization of oil sands as an unconventional fossil resource in an attempt to alleviate the energy crisis.[4]

Oil sands are a naturally occurring mixture of bitumen, clay, water, and quartz sands.[5,6] Based on their surface wettability, they can be classified into neuter-wet, water-wet, and oil-wet oil sands.[4] The organic component of oil sands is usually separated from the sand matrix using methods such as solvent extraction, hot water extraction, and pyrolysis, among others.[7] This is a necessary requirement for the utilization of oil sands.[8] Oil sands are generally characterized by high asphaltene content, carbon residue, and heteroatom content. In addition to the environmental pollution problems posed by the mining and extraction of unconventional oil reserves, the complexity associated with their geological structure makes it difficult to apply a conventional development theory to unconventional oil resources.[9,10] Hence, the need arises to employ upgrading technologies in order to produce high-value light products.[11,12]

Of the available technologies, pyrolysis is generating a lot of research interest due to its easy industrialization, wide range of application, and minimal pollution.[13] Pyrolysis is a thermochemical conversion process that involves the decomposition of an organic material in an oxygen-depleted atmosphere to generate products such as oil, gases, and char.[14] Several thermal analysis techniques including thermogravimetric analysis (TGA), differential thermal analysis, and differential scanning calorimetry can be used to obtain experimental data of pyrolysis.[13]

TGA is the most popular technique widely adopted in the estimation of pyrolysis kinetics.[15] The technique involves the weight measurement of a material subjected to heating at a known rate[7] under non-isothermal and isothermal conditions.[16] Non-isothermal analyses have been implicated to have better advantages including simulation of conditions, absence of thermal induction period, and error minimization over isothermal analyses.[17]

Many exciting studies have been carried out on estimating the pyrolysis kinetics of oil sands in recent years.[18−21] Nevertheless, many of these studies have contributed significantly to the advances in knowledge with respect to the sole use of either model-free or model-fitting method as

Received: November 19, 2022
Accepted: February 27, 2023
Published: March 9, 2023

well as the proposition of mechanistic models of chemical structure evolution during the pyrolysis of the oil resource. However, the present study represents the first known attempt at evaluating the pyrolysis characteristics of Nigerian oil sands using model-free and model-fitting methods. In the present study, TGA was used to examine the effects of different heating rates on the pyrolysis characteristics of Nigerian oil sands. The activation energies and pre-exponential factors of the oil sand pyrolysis were estimated using Kissinger−Akahira−Sunose (KAS), Starink, Simplified Arrhenius, and Coats−Redfern kinetic models. This was done with a view to provide a theoretical basis for the development of the natural resource.

2. EXPERIMENTAL SECTION

Ilubirin and Orisunbare oil sands from the oil sand bitumen deposit areas of Ondo State, Nigeria were selected for the present study. The oil sand samples were characterized using an X-ray diffractometer to estimate the mineralogical analysis. The oil sand samples were investigated under an inert atmosphere in a thermogravimetric analyzer. The model-free and model-fitting kinetic models were used to estimate the activation energy and pre-exponential factor of the process.

2.1. Sampling. Samples of oil sands were collected from Ilubirin and Orisunbare in the bitumen deposit areas of Ondo State, Nigeria. The samples were collected by scooping the viscous oil sands into hermetically sealed containers, labeled according to the names of the communities from which the samples were collected, and transported to the laboratory for various analyses.

2.2. Mineralogical Analysis. A GBC EMMA X-ray diffractometer equipment, Australia, was used to record the X-ray diffraction (XRD) spectra of samples. The measurement was taken from the goniometer scan axis in steps of 2θ, for a scan time of 38.7 s, at a temperature of 25 °C, using a Cu Kα radiation of wavelength λ = 1.5406 Å generated at 40 kV, 30 mA. Each specimen of 10 mm length was well positioned on the scan axis of the goniometer of radius 2.4×10^2 mm. The operation of the device is based on the scattering of incident X-radiation off a collection of atoms. At a given wavelength and angle of incidence of the source radiation, the scattering angle depends on the atomic row spacing, d. For scattered rays from successive atomic rows that are in phase, diffraction maxima are observable for short wavelength of the source radiation, hence the use of X-rays.[22]

2.3. Thermogravimetric Analysis. TGA was used to characterize the weight loss process of the oil sands as a function of temperature and time at different heating rates (10, 20, and 30 °C). The thermogravimetric experiments were performed using a SDT Q600 (V20.9 Build 20) DSC-TGA instrument. Throughout the experiment, nitrogen gas (99.99% purity) flow rate was 50 mL/min in order to maintain an inert atmosphere for the decomposition process, and the mass of the oil sand samples was 10 ± 0.65 mg with a particle size of 500 μm. The experiments were conducted over a temperature range of 25−600 °C.

2.4. Kinetic Modeling. The obtained TGA data was used to estimate the pyrolysis kinetics of the oil sand samples. The pyrolysis kinetic analysis is based on the Arrhenius equation and kerogen transformation rate, shown in eqs 1 and 2, respectively

$$k = k_o \cdot e^{(-E/RT)} \tag{1}$$

$$d\propto/dt = k(T)\cdot f(\propto) \tag{2}$$

where k is the rate constant, k_o is the pre-exponential factor, E is activation energy (kJ/mol), R is molar gas constant, T is temperature (in Kelvin), and α (conversion) is the standard form of weight loss and is expressed in the equation below

$$\propto = \frac{m_o - m_t}{m_o - m_f} \tag{3}$$

where m_o is the initial sample weight, m_t is the weight at a specific reaction time, and m_f is the final sample weight after pyrolysis.

The combination of eqs 1 and 2 results in eq 4 which can then be used to estimate kinetic parameters based on TGA data.

$$d\propto/dt = k_o \cdot f(\propto)\cdot e^{(-E/RT)} \tag{4}$$

$$f(\propto) = (1 - \propto)^n \tag{5}$$

Inserting eq 5 into eq 4, eq 6 is obtained

$$\frac{d\propto}{dt} = \frac{k_o}{\beta}\cdot(1 - \propto)^n \cdot e^{(-E/RT)} \tag{6}$$

In this study, four different methods comprising three isoconversional (model-free) and one model-fitting methods were employed to estimate the pyrolysis kinetics of the oil sand samples. The isoconversional methods include KAS (eq 7), Starink (eq 8), and simplified Arrhenius method (eq 9), while the model-fitting method is the Coats−Redfern method (eq 10).[23,24]

$$\ln\frac{\beta}{T^2} = \ln\left(\frac{k_0 \cdot R}{E \cdot g(\propto)}\right) - \frac{E}{RT} \tag{7}$$

$$\ln\frac{\beta}{T^{1.92}} = \ln\left(\frac{k_o \cdot E}{R \cdot g(\propto)}\right) - 1.0008\left(\frac{E}{RT}\right) \tag{8}$$

$$\ln\frac{\propto}{T^2} = \ln\left(\frac{k_o \cdot R}{E}\right) + 0.6075 - \frac{E}{RT} \tag{9}$$

$$\ln\left(\frac{g(\propto)}{T^2}\right) = \ln\left(\frac{k_0 \cdot R}{\beta \cdot E}\right) - \frac{E}{RT} \tag{10}$$

where $g(\alpha) = -\ln(1 - \alpha)$.

3. RESULTS AND DISCUSSION

3.1. Mineralogical Analysis. The mineralogical characterization of Ilubirin oil sands was carried out using XRD, and the diffraction pattern of the oil sand sample is shown in Figure 1. The diffraction pattern of Ilubirin oil sand showed obvious peaks corresponding to 20.99, 26.83, 36.73, 42.61, 50.31, 60.12, 67.88, 68.06, 68.46, and 68.64° at 2θ. The peaks are indicative of the presence of chlorite, quartz, aragonite, dolomite, calcite, and montmorillonite minerals.[25] The mineralogical analysis indicated the presence of both clay and non-clay minerals.[26] Although some studies have reported the presence of gypsum mineral in oil sands which was widely attributed to the oxidation of pyrite,[27,28] the present study could not account for the presence of gypsum mineral in the studied oil sand based on its diffraction pattern. Similarly, expandable clay minerals such as kaolinite-smectite and illite-smectite have been reported in Alberta oil sands.[29,30] However,

https://doi.org/10.1021/acsomega.2c07428
ACS Omega 2023, 8, 10111−10118

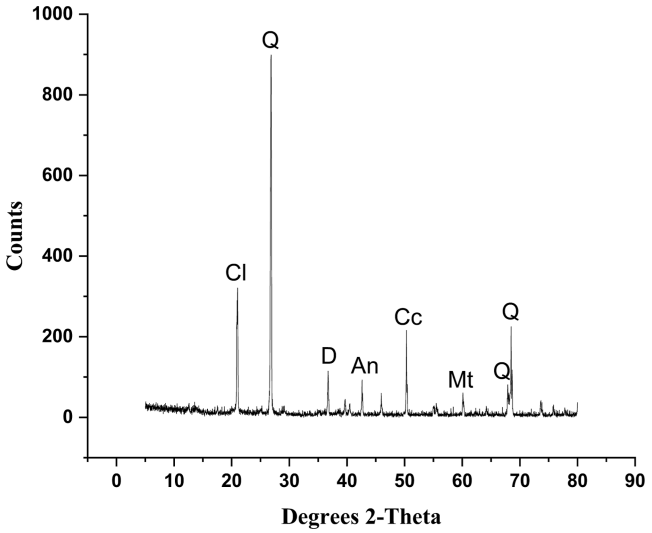

Figure 1. X-ray diffraction pattern of Ilubirin oil sand. Cl, chlorite; Q, quartz; D, dolomite; An, aragonite; Cc, calcite; Mt, montmorillonite.

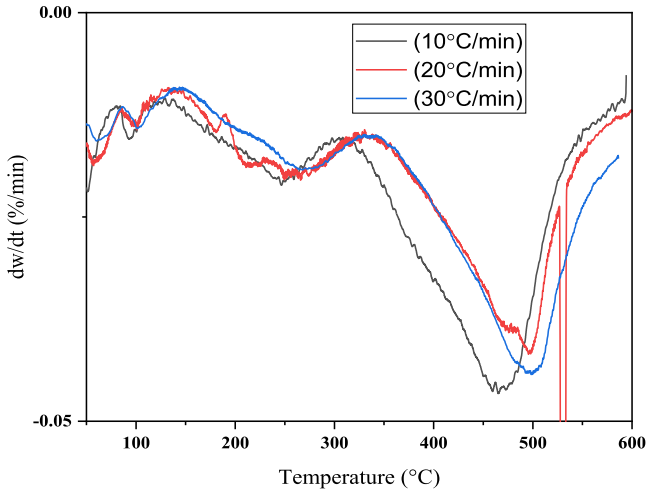

Figure 2. Differential thermogravimetry curves of Ilubirin oil sand at different heating rates.

the diffraction pattern did not show distinct peaks for these minerals in Ilubirin oil sand. This is an important finding because expandable clay minerals are known to pose enormous problems during tailings management, bitumen recovery and quality, and aqueous bitumen extraction process.[26,31] In addition to particle size, mineralogical composition makes up the two most significant factors influencing bitumen recovery.[32] The presence of clay minerals and quartz detected in the studied oil sands agrees with the findings of previous studies which reported the occurrence of the same minerals in torrefied biomass, coal, and shale samples.[33−36] The implication of this is that oil sands could be co-pyrolyzed with biomass. The minerals present in the biomass could decrease the acid content of the resulting liquid product via the inhibition of the conversion of oxygen-containing compounds and simultaneously increase the gas yield of the pyrolytic process via the promotion of C−O cracking.[37,38]

3.2. Thermogravimetric Analysis. TGA was carried out to study the pyrolysis characteristics of the oil sand samples. The representative differential thermogravimetry curve of Ilubirin oil sand at different heating rates (10, 20, and 30 °C/min) is presented in Figure 2 while the others are shown in Figures S1−S3 (Supporting Information). The varying weight loss observed in the oil sands are a reflection of the thermal decomposition of the bitumen present in the oil sands.[39] The DTG curves showed that the weight loss process of the oil sands can be separated into three steps, indicating that pyrolysis reactions occurred at three stages in both oil sand samples.[40,41] The thermogravimetric characteristics of the oil sands, showing the temperature range, weight loss, and peak temperature for the reaction regions are shown in Table S1 (Supporting Information). Only minimal variations were observed in the temperature range of the weight loss process for both oil sand samples. This could be attributed to differences emanating from geographical location of the oil sands, which might be indicative of differences in origin and composition for the native bitumen. At all heating rates, the first region occurring between 25 and 145 °C is called the low-temperature oxidation region.[39] In this region, inter-layer water from clay minerals, moisture, and low volatility substances vaporized from the oil sand samples. The highest weight loss observed in Ilubirin oil sand in this region was 1.65 wt % at 20 °C/min, while that of Orisunbare oil sand was 1.15 wt % at 30 °C/min. The weight loss observed in this region for both oil sand samples was not significant due to the low moisture content. The second region occurring between 102 and 394 °C is called the devolatilization region.[42] In this region, the desorption and volatilization of light organics occur without coking.[40,43] The highest weight loss observed in Ilubirin oil sand in this region was 3.05 wt % at 20 °C/min, while it was 9.92 wt % at 10 °C/min in Orisunbare oil sand. The third region occurring between 310 and 584 °C is called the high-temperature oxidation region.[39] In this region, the thermal cracking of heavy hydrocarbons is the predominant reaction occurring. Here, heavy organics are broken down into oil and gaseous hydrocarbons.[44] The highest weight loss observed in Ilubirin oil sand in this region was 6.33 wt % at 30 °C/min, while that of Orisunbare oil sand was 3.51 wt % at 10 °C/min. The third region was the most pronounced peak on the DTG curve, indicating that the major pyrolytic process occurs within this region.

The heating rates had significant effects on the thermal decomposition of the oil sands. A shift in the reaction region to higher temperatures with increase in heating rate was observed in both oil sand samples. In addition, the peak temperature was observed to rise with increasing heating rate. This can be explained in terms of medium diffusion and heat transfer.[43,45] This important observation is probably due to harsher conditions at higher heating rates, which subsequently results in complete pyrolysis at higher temperatures.[44] As reported in studies that explored the pyrolysis of biomass and other polymeric materials,[46,47] these shifts are known as thermal lag or thermal hysteresis.[48] Upon increased heating rates, there was an upsurge in the temperature gradient between the exterior and interior of the oil sands. This resulted in the enhancement of the degree of diffusion control, leading to the initiation of secondary reactions.[49]

3.3. Differential Scanning Calorimetry. The differential scanning calorimetry (DSC) curves of Ilubirin and Orisunbare oil sands at different heating rates are shown in Figures 3 and 4 respectively. The two curves are characterized by endothermic peaks, followed by pronounced exothermic peaks and then another endothermic peak. The endothermic peaks correspond to the low-temperature oxidation and high-temperature

https://doi.org/10.1021/acsomega.2c07428
ACS Omega 2023, 8, 10111−10118

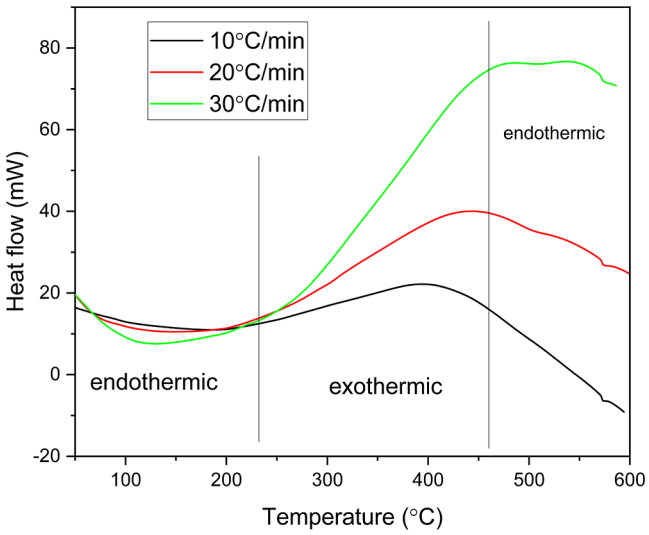

Figure 3. Differential scanning calorimetry curves of Ilubirin oil sand at different heating rates.

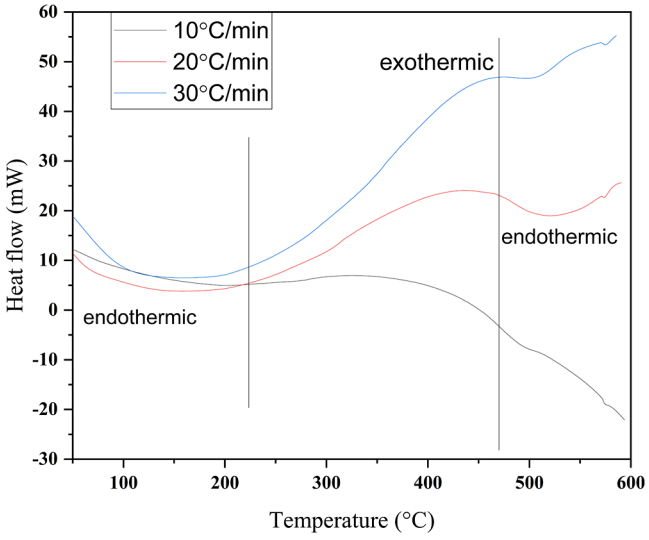

Figure 4. Differential scanning calorimetry curves of Orisunbare oil sand at different heating rates.

oxidation regions, while the exothermic peak corresponds to the devolatilization region.[39,50] A notable observation in the DSC curves of both oil sand samples is the shift to higher temperature with increasing heating rate. This is an indication that endothermicity of the pyrolytic process increases with increasing heating rate.

3.4. Pyrolysis Kinetics. The use of TGA represents one of the reliable approaches to determine the kinetics of pyrolysis. The kinetics of pyrolysis are based on the Arrhenius equation.[24] The kinetic methods of analysis employed are Coats−Redfern, KAS, Starink, and Arrhenius methods. The evaluated methods were adopted in the form of a linear relationship with reciprocal temperature $(1/T)$. For each degree of conversion, the models are shown in Figures S4−S7 (Supporting Information); the calculated activation energy and pre-exponential factor for Ilubirin oil sand are presented in Tables 1 and 2 while those for Orisunbare oil sand are presented in Tables S2 and S3 (Supporting Information). Each value of the activation energy presented depicts a weighted average of a distribution of activation energies.[51,52] The correlation coefficients obtained from the linear regression analysis showed that the Coats−Redfern and Arrhenius method has R^2 values generally greater than 0.999 for the studied oil sands. There were significant variations in the R^2 values obtained from the linear regression analysis of the KAS and Starink methods. The Coats−Redfern and Arrhenius methods showed that activation energy increases with increasing degree of conversion. For the Ilubirin oil sands, the KAS and Starink methods were sensitive to fluctuations in the activation energy at $0.20 \leq \alpha \leq 0.30$ and $0.20 \leq \alpha \leq 0.50$, respectively. For the Orisunbare oil sands, the KAS and Starink methods were sensitive to fluctuations in the activation energy at $0.35 \leq \alpha \leq 0.85$. The observed fluctuation of activation energy of the oil sands with the degree of conversion is in agreement with the findings of refs 49 and 53, and this was attributed to the complexity of multiple pyrolysis reactions in the oil sand.[49] The difference in the activation energies of the two oil sand samples is directly connected to their different mineral and organic compositions. Hence, the higher the volatile content, the more prone it was to thermal reaction.[53] Lower activation energies were obtained for KAS and Starink methods compared to the Coats−Redfern and Arrhenius methods. The activation energies of the studied oil sands were lower than those reported in Athabasca oil sand bitumen,[54] Kazakhstan oil sand,[43] Tumuji oil sand,[40] Alberta oil sand,[55] and Karamay oil sand.[56] This variation may be attributed to discrepancies in the properties of the oil sands.

The conversion dependence of the activation energies obtained by the isoconversional methods is presented in Figure 5. Evidently, there was an increase in activation energy with increasing degree of conversion. This is a reflection of the observed increase in conversion at higher temperatures during TGA.[24] At low degree of conversion, the reaction was predominantly the cleavage of weak chemical bonds and volatilization of low-boiling components. However, the pyrolysis process required higher energy to promote the cleavage of shorter alkyl side chains that may have originated from the dehydrogenation of naphthenic rings, ring-opening reaction, and the cracking of long side chains at higher degree of conversion.[12] During TGA, the detection of conversion is predominantly linked with the detection of weight loss. This is a limitation in the use of TGA for estimating the pyrolysis kinetics of oil sands because reactions resulting in the formation of non-volatile oil products and coke-like residue at a particular temperature would be disregarded as weight losses. Based on the Arrhenius method that gave the best fit among the isoconversional methods, the conversion dependence of the activation energy was regressed as a third-order polynomial and eqs 11 and 12 were obtained for activation energy and pre-exponential factor, respectively.

$$E = 15.617 \cdot \alpha^3 - 29.613 \cdot \alpha^2 + 24.800 \cdot \alpha + 4.202 \quad (11)$$

$$\ln K_0 = 6.61 \times 10^{-8} \cdot \alpha^3 - 2.43 \times 10^{-7} \cdot \alpha^2 + 2.91 \times 10^{-7} \cdot \alpha + 6.01 \times 10^{-8} \quad (12)$$

The correlation coefficients of activation energy and pre-exponential factor were 0.99 and 0.96, respectively. The good correlation between pre-exponential factor and activation energy, as functions of conversion, is indicative of kinetic compensation effect.[57]

https://doi.org/10.1021/acsomega.2c07428
ACS Omega 2023, 8, 10111−10118

Table 1. Calculated Activation Energy (kJ mol^{-1}) and Pre-exponential Factor (min^{-1}) for Pyrolysis Reaction of Ilubirin Oil Sand[a]

	Coats−Redfern			Kissinger−Akahira−Sunose		
α	E_a	K_0	R^2	E_a	K_0	R^2
0.05	5.334	6.732×10^{-8}	0.999	1.020	1.722×10^{-3}	0.366
0.10	6.532	9.241×10^{-8}	0.999	3.965	5.63×10^{-4}	0.696
0.15	7.391	1.113×10^{-7}	0.999	4.338	4.55×10^{-4}	0.731
0.20	8.041	1.291×10^{-7}	0.999	3.898	4.7×10^{-4}	0.657
0.25	8.681	1.428×10^{-7}	0.999	3.907	4.36×10^{-4}	0.622
0.30	9.163	1.586×10^{-7}	0.999	4.999	3.22×10^{-4}	0.678
0.35	9.830	1.668×10^{-7}	0.999	7.065	1.99×10^{-4}	0.753
0.40	10.356	1.782×10^{-7}	0.999	7.719	1.69×10^{-4}	0.767
0.45	10.968	1.859×10^{-7}	0.999	7.430	1.74×10^{-4}	0.767
0.50	11.203	2.066×10^{-7}	0.999	7.505	1.68×10^{-4}	0.788
0.55	11.627	2.21×10^{-7}	0.999	7.691	1.59×10^{-4}	0.798
0.60	11.865	2.435×10^{-7}	0.999	7.904	1.51×10^{-4}	0.801
0.65	12.165	2.655×10^{-7}	0.999	8.127	1.43×10^{-4}	0.803
0.70	12.469	2.898×10^{-7}	0.999	8.501	1.33×10^{-4}	0.812
0.75	12.588	3.273×10^{-7}	0.999	9.346	1.15×10^{-4}	0.842
0.80	12.570	3.811×10^{-7}	1	9.618	1.09×10^{-4}	0.842
0.85	13.323	3.997×10^{-7}	0.999	11.386	8.26×10^{-5}	0.908
0.9	13.892	4.455×10^{-7}	0.999	13.033	6.42×10^{-5}	0.956
0.95	14.682	5.183×10^{-7}	0.999	14.312	5.33×10^{-5}	0.974

[a]α = degree of conversion.

Table 2. Calculated Activation Energy (kJ mol^{-1}) and Pre-exponential Factor (min^{-1}) for Pyrolysis Reaction of Ilubirin Oil Sand[a]

	Starink			Arrhenius		
α	E_a	K_0	R^2	E_a	K_0	R^2
0.05	0.792	2.976×10^{-3}	0.292	5.344	6.54×10^{-8}	0.999
0.10	3.703	9.83×10^{-4}	0.671	6.533	8.77×10^{-8}	0.999
0.15	4.041	8.03×10^{-4}	0.707	7.395	1.03×10^{-7}	0.999
0.20	3.574	8.35×10^{-4}	0.624	8.046	1.16×10^{-7}	0.999
0.25	3.561	7.8×10^{-4}	0.587	8.677	1.24×10^{-7}	0.999
0.30	4.632	5.79×10^{-4}	0.649	9.173	1.33×10^{-7}	0.999
0.35	6.672	3.6×10^{-4}	0.734	9.83	1.36×10^{-7}	0.999
0.40	7.300	1.49×10^{-4}	0.749	10.381	1.39×10^{-7}	0.999
0.45	6.993	3.17×10^{-4}	0.748	10.957	1.4×10^{-7}	0.999
0.50	7.053	3.06×10^{-4}	0.769	11.235	1.48×10^{-7}	0.999
0.55	7.226	2.91×10^{-4}	0.780	11.631	1.52×10^{-7}	0.999
0.60	7.427	2.77×10^{-4}	0.783	11.891	1.59×10^{-7}	0.999
0.65	7.639	2.63×10^{-4}	0.785	12.18	1.64×10^{-7}	0.999
0.70	8.003	2.45×10^{-4}	0.795	12.46	1.69×10^{-7}	0.999
0.75	8.837	2.12×10^{-4}	0.828	12.657	1.75×10^{-7}	0.999
0.80	9.100	2.02×10^{-4}	0.828	12.795	1.83×10^{-7}	0.999
0.85	10.852	1.53×10^{-4}	0.900	13.331	1.79×10^{-7}	0.999
0.9	12.477	1.19×10^{-4}	0.952	13.907	1.74×10^{-7}	0.999
0.95	13.726	9.93×10^{-5}	0.972	14.642	1.65×10^{-7}	0.999

[a]α = degree of conversion.

4. CONCLUSIONS

The pyrolysis characteristics of Nigerian oil sands were studied using TGA. The pyrolysis process showed that there were three main stages comprising low-temperature oxidation, devolatilization, and high-temperature oxidation. The low-temperature oxidation stage involves the loss of inter-layer water and low volatility substances, the devolatilization stage involves the volatilization of light organics without coking, while the high-temperature oxidation involves the thermal cracking of heavy hydrocarbons into lighter oil and gaseous hydrocarbons. The peak temperature increased with increasing heating rate. Mineralogical analysis showed the notable absence of expandable clay minerals, indicating that little or no problems should be encountered during the tailings management and aqueous bitumen extraction process of the studied oil sands. Kinetic models comprising KAS, Starink, simplified Arrhenius, and Coats−Redfern were used to estimate the activation energy and pre-exponential factor. The kinetic parameters showed good correlation which indicated kinetic compensation effect. The Coats−Redfern model exhibited the best model fit for describing the pyrolysis

https://doi.org/10.1021/acsomega.2c07428
ACS Omega 2023, 8, 10111−10118

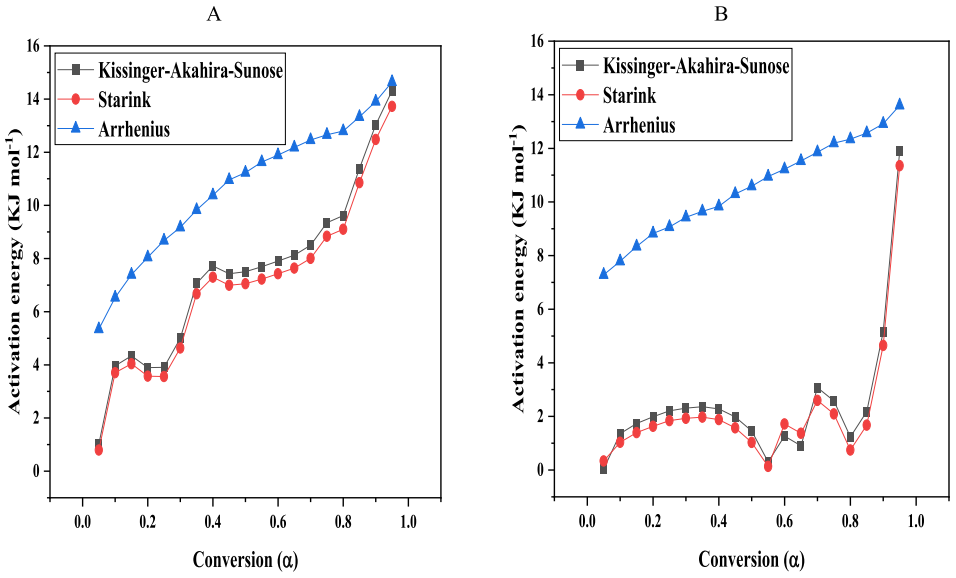

Figure 5. Plots of calculated activation energies from isoconversional methods as a function of conversion. (A) Ilubirin oil sand (B) Orisunbare oil sand.

process of Nigerian oil sands. Our results showed that the relatively low activation energies and the absence of clay minerals can dramatically make the Nigerian oil sands to be a valuable energy resource in the face of dwindling conventional oil reserves. The findings of the study provided a scientific basis for explaining the conversion-dependent change in activation energy. The study represents the first known attempt at providing important scientific information required for the exploration of the natural resource.

■ ASSOCIATED CONTENT

Supporting Information

The Supporting Information is available free of charge at https://pubs.acs.org/doi/10.1021/acsomega.2c07428.

Thermogravimetry and differential thermogravimetry curves as well as kinetic analysis of TGA data; thermogravimetric characteristics; calculated activation energies; and pre-exponential factors (PDF)

■ AUTHOR INFORMATION

Corresponding Author

Odunayo T. Ore − *Department of Chemistry, Obafemi Awolowo University, Ile-Ife 220005, Nigeria;* orcid.org/0000-0002-5529-1509; Email: oreodunayo@yahoo.com, oreodunayo@gmail.com

Author

Festus M. Adebiyi − *Department of Chemistry, Obafemi Awolowo University, Ile-Ife 220005, Nigeria*

Complete contact information is available at: https://pubs.acs.org/10.1021/acsomega.2c07428

Notes

The authors declare no competing financial interest.

The data analyzed and/or generated during the study will be made available upon reasonable request from the corresponding author.

All authors have approved the final version of the manuscript for publication.

■ ACKNOWLEDGMENTS

The authors sincerely acknowledge the management of Obafemi Awolowo University, Ile-Ife, Nigeria, for providing an enabling environment for the research.

■ REFERENCES

(1) De Silva, P.; Simons, S.; Stevens, P. Economic impact analysis of natural gas development and the policy implications. *Energy Pol.* **2016**, *88*, 639−651.

(2) Ajumobi, O. O.; Muraza, O.; Kondoh, H.; Hasegawa, N.; Nakasaka, Y.; Yoshikawa, T.; Al Amer, A. M.; Masuda, T. Upgrading oil sand bitumen under superheated steam over ceria-based nanocomposite catalysts. *Appl. Energy* **2018**, *218*, 1−9.

(3) Hua, Z.; Wang, Q.; Jia, C.; Liu, Q. Pyrolysis kinetics of a Wangqing oil shale using thermogravimetric analysis. *Energy Sci. Eng.* **2019**, *7*, 912−920.

(4) Wang, T.; Zhang, C.; Zhao, R.; Zhu, C.; Yang, C.; Liu, C. Solvent extraction of bitumen from oil sands. *Energy Fuel.* **2014**, *28*, 2297−2304.

(5) Ore, O. T.; Adeola, A. O. Toxic metals in oil sands: review of human health implications, environmental impact, and potential remediation using membrane-based approach. *Energy Ecol. Environ.* **2021**, *6*, 81−91.

(6) Adebiyi, F. M.; Ore, O. T. EDXRF analysis and risks assessment of potentially toxic elements in sand fraction (tailing) of Nigerian oil sands. *Energy Ecol. Environ.* **2021**, *6*, 258−270.

(7) Jia, C.; Wang, Z.; Liu, H.; Bai, J.; Chi, M.; Wang, Q. Pyrolysis behavior of Indonesia oil sand by TG-FTIR and in a fixed bed reactor. *J. Anal. Appl. Pyrol.* **2015**, *114*, 250−255.

(8) La, H.; Guigard, S. E. Extraction of hydrocarbons from Athabasca oil sand slurry using supercritical carbon dioxide. *J. Supercrit. Fluids* **2015**, *100*, 146−154.

(9) Esterhuyse, S. Identifying the risks and opportunities of unconventional oil and gas extraction using the strategic environmental assessment. *Curr. Opin. Environ. Sci. Health* **2018**, *3*, 33−39.

(10) Song, Y.; Zhuo, L.; Jiang, Z.; Qun, L.; Dongdong, L.; Zhiye, G. Progress and development trend of unconventional oil and gas geological research. *Petrol. Explor. Dev.* **2017**, *44*, 675−685.

(11) Morimoto, M.; Sugimoto, Y.; Sato, S.; Takanohashi, T. Comparison of thermal cracking processes for Athabasca oil sand bitumen: Relationship between conversion and yield. *Energy Fuel.* **2014**, *28*, 6322−6325.

(12) Hao, J.; Che, Y.; Tian, Y.; Li, D.; Zhang, J.; Qiao, Y. Thermal cracking characteristics and kinetics of oil sand bitumen and its SARA fractions by TG−FTIR. *Energy Fuels* **2017**, *31*, 1295−1309.
(13) Jia, C.; Chen, J.; Bai, J.; Yang, X.; Song, S.; Wang, Q. Kinetics of the pyrolysis of oil sands based upon thermogravimetric analysis. *Thermochim. Acta* **2018**, *666*, 66−74.
(14) Ore, O. T.; Adebiyi, F. M. A review on current trends and prospects in the pyrolysis of heavy oils. *J. Pet. Explor. Prod. Technol.* **2021**, *11*, 1521−1530.
(15) Jia, C.; Wang, Q.; Ge, J.; Xu, X. Pyrolysis and combustion model of oil sands from non-isothermal thermogravimetric analysis data. *J. Therm. Anal. Calorim.* **2014**, *116*, 1073−1081.
(16) Ahmad, M. S.; Mehmood, M. A.; Al Ayed, A.; Luo, G.; Ibrahim, H.; Rashid, M.; Arbi Nehdi, U.; Qadir, I. A.; Qadir, G. Kinetic analyses and pyrolytic behavior of Para grass (Urochloa mutica) for its bioenergy potential. *Bioresour. Technol.* **2017**, *224*, 708−713.
(17) Abu El-Rub, Z.; Kujawa, J.; Al-Gharabli, S. Pyrolysis kinetic parameters of Omari oil shale using thermogravimetric analysis. *Energies* **2020**, *13*, 4060.
(18) Wang, Z.; Wang, Q.; Jia, C.; Bai, J. Thermal evolution of chemical structure and mechanism of oil sands bitumen. *Energy* **2022**, *244*, 123190.
(19) Wang, Z.; Wang, Q.; Jia, C.; Bai, J. Structure characteristics and evolution mechanism of oil sands bitumen at Karamay, Xinjiang (China). *J. Petrol. Sci. Eng.* **2022**, *214*, 110421.
(20) Li, S.; Lu, B.; Lin, X.; Zhou, Y.; Song, J.; Wang, Y. The rapid pyrolysis feature and evolution of heteroatoms of Indonesian oil sand. *J. Anal. Appl. Pyrol.* **2022**, *165*, 105537.
(21) Jia, C.; Yu, H.; Liu, H.; Qin, H.; Wang, Q. Pyrolysis Characteristics of Indonesian Oil Sand in a Fixed Bed. *ACS Omega* **2022**, *7*, 23315−23321.
(22) Park, R. L.; Lagally, M. G. *Solid State Physics: Surfaces*; Academic Press, 1985.
(23) Zhao, H.-y.; Cao, Y.; Sit, S. P.; Lineberry, Q.; Pan, W.-p. Thermal characteristics of bitumen pyrolysis. *J. Therm. Anal. Calorim.* **2012**, *107*, 541−547.
(24) Foltin, J. P.; Lisboa, A. C. L.; de Klerk, A. Oil shale pyrolysis: Conversion dependence of kinetic parameters. *Energy Fuels* **2017**, *31*, 6766−6776.
(25) Han, D. Y.; Yu, W.; Luo, K.; Cao, Z. Study on the process of oil recovery from oil sludge and tailing oil sands by blending extraction. *Pet. Sci. Technol.* **2019**, *37*, 2269.
(26) Geramian, M.; Ivey, D. G.; Liu, Q.; Etsell, T. H. Characterization of four petrologic end members from Alberta oil sands and comparison between different mines and sampling times. *Can. J. Chem. Eng.* **2018**, *96*, 49−61.
(27) Todd, E.; Sherman, D.; Purton, J. Surface oxidation of pyrite under ambient atmospheric and aqueous (pH= 2 to 10) conditions: electronic structure and mineralogy from X-ray absorption spectroscopy. *Geochim. Cosmochim. Acta* **2003**, *67*, 881−893.
(28) Honty, M.; De Craen, M.; Wang, L.; Madejová, J.; Czímerová, A.; Pentrák, M.; Stríček, I.; Van Geet, M. The effect of high pH alkaline solutions on the mineral stability of the Boom Clay−Batch experiments at 60 C. *Appl. Geochem.* **2010**, *25*, 825−840.
(29) Adeyinka, O. B.; Samiei, S.; Xu, Z.; Masliyah, J. H. Effect of particle size on the rheology of Athabasca clay suspensions. *Can. J. Chem. Eng.* **2009**, *87*, 422−434.
(30) Kaminsky, H. A.; Etsell, T. H.; Ivey, D. G.; Omotoso, O. Distribution of clay minerals in the process streams produced by the extraction of bitumen from Athabasca oil sands. *Can. J. Chem. Eng.* **2009**, *87*, 85−93.
(31) Smith, R. G.; Schramm, L. L. The influence of mineral components on the generation of natural surfactants from Athabasca oil sands in the alkaline hot water process. *Fuel Process. Technol.* **1992**, *30*, 1−14.
(32) Wik, S.; Sparks, B.; Ng, S.; Tu, Y.; Li, Z.; Chung, K.; Kotlyar, L. Effect of process water chemistry and particulate mineralogy on model oilsands separation using a warm slurry extraction process simulation. *Fuel* **2008**, *87*, 1394−1412.
(33) Karayigit, A. I.; Bircan, C.; Oskay, R. G.; Türkmen, İ.; Querol, X. The geology, mineralogy, petrography, and geochemistry of the Miocene Dursunbey coal within fluvio-lacustrine deposits, Balıkesir (Western Turkey). *Int. J. Coal Geol.* **2020**, *228*, 103548.
(34) Karayigit, A. I.; Atalay, M.; Oskay, R. G.; Córdoba, P.; Querol, X.; Bulut, Y. Variations in elemental and mineralogical compositions of Late Oligocene, Early and Middle Miocene coal seams in the Kale-Tavas Molasse sub-basin, SW Turkey. *Int. J. Coal Geol.* **2020**, *218*, 103366.
(35) Trubetskaya, A.; Jensen, P. A.; Jensen, A. D.; Steibel, M.; Spliethoff, H.; Glarborg, P.; Larsen, F. H. Comparison of high temperature chars of wheat straw and rice husk with respect to chemistry, morphology and reactivity. *Biomass Bioenergy* **2016**, *86*, 76−87.
(36) Trubetskaya, A.; Leahy, J. J.; Yazhenskikh, E.; Müller, M.; Layden, P.; Johnson, R.; Ståhl, K.; Monaghan, R. F. Characterization of woodstove briquettes from torrefied biomass and coal. *Energy* **2019**, *171*, 853−865.
(37) Chen, B.; Han, X.; Mu, M.; Jiang, X. Studies of the co-pyrolysis of oil shale and wheat straw. *Energy Fuels* **2017**, *31*, 6941−6950.
(38) Li, R.; Zhong, Z.; Jin, B.; Zheng, A. Application of mineral bed materials during fast pyrolysis of rice husk to improve water-soluble organics production. *Bioresour. Technol.* **2012**, *119*, 324−330.
(39) Sonibare, O.; Egashira, R.; Adedosu, T. Thermo-oxidative reactions of Nigerian oil sand bitumen. *Thermochim. Acta* **2003**, *405*, 195−205.
(40) Meng, M.; Hu, H.; Zhang, Q.; Li, X.; Wu, B. Pyrolysis behaviors of Tumuji oil sand by thermogravimetry (TG) and in a fixed bed reactor. *Energy Fuel.* **2007**, *21*, 2245−2249.
(41) Wang, Q.; Jia, C.; Jiang, Q.; Wang, Y.; Wu, D. Pyrolysis model of oil sand using thermogravimetric analysis. *J. Therm. Anal. Calorim.* **2014**, *116*, 499−509.
(42) Nie, F.; He, D.; Guan, J.; Li, X.; Hong, Y.; Wang, L.; Zheng, H.; Zhang, Q. Oil sand pyrolysis: Evolution of volatiles and contributions from mineral, bitumen, maltene, and SARA fractions. *Fuel* **2018**, *224*, 726−739.
(43) Fan, Q.; Bai, G.; Wu, S.; Yuan, W.; Song, X.-M. The chemical structure and the kinetics research of oil-wet oil sand from Kazakhstan during pyrolysis process. *Pet. Sci. Technol.* **2017**, *35*, 1495−1501.
(44) Gao, J.; Xu, T.; Wang, G.; Zhang, A.; Xu, C. Reaction behavior of oil sand in fluidized-bed pyrolysis. *Petrol. Sci.* **2013**, *10*, 562−570.
(45) Zhang, C.; Jiang, X.; Wei, L.; Wang, H. Research on pyrolysis characteristics and kinetics of super fine and conventional pulverized coal. *Energy Convers. Manage.* **2007**, *48*, 797−802.
(46) Quan, C.; Gao, N.; Song, Q. Pyrolysis of biomass components in a TGA and a fixed-bed reactor: Thermochemical behaviors, kinetics, and product characterization. *J. Anal. Appl. Pyrol.* **2016**, *121*, 84−92.
(47) Gao, N.; Quan, C.; Ma, Z.; Wu, C. Thermal characteristics of biomass pyrolysis oil and potential hydrogen production by catalytic steam reforming. *Energy Fuels* **2018**, *32*, 5234−5243.
(48) Ma, Z.; Xie, J.; Gao, N.; Quan, C. Pyrolysis behaviors of oilfield sludge based on Py-GC/MS and DAEM kinetics analysis. *J. Energy Inst.* **2019**, *92*, 1053−1063.
(49) Han, J.; Sun, Y.; Guo, W.; Deng, S.; Hou, C.; Qu, L.; Li, Q. Non-isothermal thermogravimetric analysis of pyrolysis kinetics of four oil shales using Sestak−Berggren method. *J. Therm. Anal. Calorim.* **2019**, *135*, 2287−2296.
(50) Kuang, W.; Lu, M.; Yeboah, I.; Qian, G.; Duan, X.; Yang, J.; Chen, D.; Zhou, X. A comprehensive kinetics study on non-isothermal pyrolysis of kerogen from Green River oil shale. *Chem. Eng. J.* **2019**, *377*, 120275.
(51) Li, S.; Yue, C. Study of pyrolysis kinetics of oil shale. *Fuel* **2003**, *82*, 337−342.
(52) Petersen, H. I.; Bojesen-Koefoed, J. A.; Mathiesen, A. Variations in composition, petroleum potential and kinetics of Ordovician−Miocene type i and type i-ii source rocks (oil shales): implications for hydrocarbon generation characteristics. *J. Petrol. Geol.* **2010**, *33*, 19−41.

https://doi.org/10.1021/acsomega.2c07428
ACS Omega 2023, 8, 10111−10118

(53) Bai, F.; Sun, Y.; Liu, Y.; Li, Q.; Guo, M. Thermal and kinetic characteristics of pyrolysis and combustion of three oil shales. *Energy Convers. Manage.* **2015**, *97*, 374−381.
(54) Shin, S.; Im, S. I.; Kwon, E. H.; Na, J.-G.; Nho, N. S.; Lee, K. B. Kinetic study on the nonisothermal pyrolysis of oil sand bitumen and its maltene and asphaltene fractions. *J. Anal. Appl. Pyrol.* **2017**, *124*, 658−665.
(55) Park, Y. C.; Paek, J.-Y.; Bae, D.-H.; Shun, D. Study of pyrolysis kinetics of Alberta oil sand by thermogravimetric analysis. *Kor. J. Chem. Eng.* **2009**, *26*, 1608−1612.
(56) Luo, M. Y.; Xia, D.; Liu, W.; Liu, X. A study on the thermogravimetric characters of oil sands and its application to thermal oil extracting system. *Boil Manuf.* **2007**, *1*, 73−76.
(57) Janković, B. The kinetic modeling of the non-isothermal pyrolysis of Brazilian oil shale: Application of the Weibull probability mixture model. *J. Petrol. Sci. Eng.* **2013**, *111*, 25−36.

https://doi.org/10.1021/acsomega.2c07428
ACS Omega 2023, 8, 10111−10118